Electrophysiological properties of electrical synapses between rat sympathetic preganglionic neurones *in vitro*

Matthew F. Nolan, Stephen D. Logan and David Spanswick

Department of Biomedical Sciences, University of Aberdeen, Foresterhill, Aberdeen AB25 2ZD, UK

1. The electrophysiological properties of electrical synaptic transmission between sympathetic preganglionic neurones (SPNs) in slices of rat spinal cord were investigated using simultaneous dual-electrode patch-clamp recordings. Electrotonic coupling was directly demonstrated between 21 pairs of SPNs.

2. Coupling coefficients determined from the steady-state response of both neurones to current steps injected into either neurone ranged from 0·02 to 0·48 (0·18 ± 0·02, mean ± S.E.M.). Synapses were bidirectional and symmetrical for the majority of connections with coupling coefficients similar in either direction. Asymmetrical coupling between a minority of cell pairs was due to differences in passive neuronal properties rather than rectification of the synaptic conductances.

3. Action potentials were manifest in adjoining cells as biphasic electrical postsynaptic potentials (ePSPs), composed of a rapid depolarising component followed by a more prolonged hyper-polarisation with amplitudes of 1·2 ± 0·2 and 2·1 ± 0·6 mV, respectively.

4. Postsynaptic potentials resembled low-pass filtered presynaptic spikes with frequency dependence determined by the junctional conductance and postsynaptic membrane properties. Increases in presynaptic action potential frequency caused attenuation of the hyper-polarising component of the ePSP that was attributed to shorter duration presynaptic spikes being more markedly filtered.

5. Synchronisation of spontaneous action potentials between electrotonically coupled neurones was driven by subthreshold membrane potential activity resembling repetitive ePSPs. Synchronous spike firing in previously silent neurones could be driven by suprathreshold ePSPs induced by suprathreshold depolarisation of a single adjoining neurone.

6. These data characterise reliable communication of sub- and suprathreshold activity by electrical synapses enabling synchronised SPN firing which may contribute to generation of coherent sympathetic rhythms and promote summation of inputs to postganglionic neurones.

Sympathetic preganglionic neurones (SPNs) mediate the central sympathetic output to postganglionic neurones in peripheral ganglia which in turn innervate target organs (Janig & McLachlan, 1992). The discharge of pre- and post-ganglionic sympathetic nerves *in vivo* includes synchronous rhythmic components which occur at frequencies of < 0·5 Hz, 2–6 Hz and approximately 10 Hz (Gebber, 1980; McAllen & Malpas, 1997; Malpas, 1998). Synchronisation of preganglionic activity may be required to enable summation of weak inputs to threshold for firing of postganglionic neurones (Janig & McLachlan, 1992). Recordings of synchronous action potentials and subthreshold membrane potential oscillations from electrotonically coupled SPNs *in vitro*, suggest that electrical synapses between SPNs may contribute to generation of synchronous rhythmic patterns

of sympathetic activity (Logan *et al.* 1996). However, an understanding of the cellular electrophysiological properties of electrical synaptic transmission between SPNs is necessary in order to determine how they may contribute to sympathetic output.

Electrical synapses formed by gap junctions between neurones mediate intercellular communication by allowing electrotonic flow of current directly from a presynaptic to a postsynaptic neurone (Llinás, 1985; Jefferys, 1995; Bennett, 1997). Electrophysiological and anatomical studies suggest the existence of electrical synapses between neurones in the hippocampus, inferior olive, locus coeruleus, hypothalamus, and spinal cord (Llinás, 1985; Jefferys, 1995; Dermietzel, 1996). Electrical synapses allow reciprocal transfer of currents between neurones and may therefore be able to

mediate synchronisation of neuronal activity. For example, in the inferior olive, subthreshold membrane potential oscillations are synchronised by electrotonic coupling between neurones resulting in synchronisation of climbing fibre inputs to cerebellar Purkinje cells (Llinás, 1985; Welsh & Llinás, 1997) and, in the hippocampus, axo-axonic coupling may mediate synchronised rhythmic action potential firing (Draguhn et al. 1998).

In contrast to chemical synaptic transmission, the transfer of information between mammalian neurones by electrical synapses is not well characterised. Properties such as the junctional conductance, voltage dependence, rectification, postsynaptic response to presynaptic action potentials and contribution of individual neurones to synchronous network activity have been investigated using invertebrate and lower vertebrate preparations (Bennett, 1977, 1997) and by modelling electrotonically coupled neurones (Traub, 1995; Vigmond et al. 1997; Marder, 1998), but have not been examined directly at electrical synapses between mammalian neurones.

In the present study we have focused on characterising these properties for electrical synapses between SPNs and on how the synaptic properties may contribute to the generation of synchronous neuronal activity. A preliminary account of part of this work has been published (Nolan et al. 1998).

METHODS

Electrophysiological recordings were made from transverse thoracolumbar spinal cord slices as described previously (Pickering et al. 1991; Logan et al. 1996). Sprague–Dawley rats, aged 8–14 days, were anaesthetised with Enflurane (7 % in O_2; Abbott laboratories, Kent, UK), killed by decapitation and the spinal cord removed and cut into slices (300–500 μm thick) using a vibratome (Intracel Series 1000, Royston, UK). Slices were maintained in artificial cerebrospinal fluid (ACSF) at 32–35 °C for 1 h after cutting and then at room temperature (18–23 °C). For recording, individual slices were held between two grids in a chamber continuously perfused with ACSF (4–8 ml min^{-1}), illuminated from below and viewed under a dissection microscope. The ACSF was of the following composition (mM): NaCl, 127; KCl, 1·9; KH$_2$PO$_4$, 1·2; CaCl$_2$, 2·4; MgCl$_2$, 1·3; NaHCO$_3$, 26; D-glucose, 10; equilibrated with 95 % O_2–5 % CO_2.

Whole-cell recordings were made from neurones in the region of the intermediolateral nucleus with either EPC-7 (List-medical) or Axopatch-1D (Axon Instruments) amplifiers, using the 'blind' version of the patch-clamp technique (Pickering et al. 1991). Patch pipettes were pulled from thin-walled borosilicate glass (GC150-TF10, Clarke Electromedical, Pangbourne, UK) and had resistances of 3–8 MΩ when filled with intracellular solution of the following composition (mM): potassium gluconate, 130; KCl, 10; MgCl$_2$, 2; CaCl$_2$, 1; EGTA-Na, 1; Hepes, 10; Na$_2$ATP, 2; and either Lucifer Yellow, 2 or biocytin, 5; pH adjusted to 7·4 with KOH, osmolarity adjusted to 315 mosmol l^{-1} with sucrose. Series resistances were in the range 8–50 MΩ and were compensated appropriately. Recordings were made simultaneously from pairs of neurones in current-clamp mode. SPNs were identified by their characteristic electrophysiological properties (Pickering et al. 1991; Logan et al.

1996). Electrotonic coupling between neurones was detected by observation of a membrane potential change in one neurone following a membrane polarisation induced by injection of current into the other neurone. If coupling could not be demonstrated one electrode was withdrawn, replaced and recordings made from another cell, until a coupled pair of neurones was found. Recordings were occasionally made from SPNs simultaneously with presumed spinal interneurones; however, no evidence for chemical or electrical coupling was observed from these pairs.

Current and voltage data were displayed on-line with a digital oscilloscope (Gould DSO1602), and stored on DAT tape (Biologic DTR-1205, Intracel, Royston, UK). In addition, data were filtered at 3–5 kHz, digitised at 10–20 kHz (Digidata 1200A board, Axon Instruments) and stored on a personal computer running pCLAMP 7 software (Axon Instruments) or Spike 2 (Cambridge Electronic Design). Analysis of electrophysiological data was carried out using Axograph3 software on a Macintosh Power PC (8100/80, Apple) or Spike 2 on a PC. Statistical analysis was carried out using Statistica 4.1 (StatSoft). All values are given as means ± S.E.M. Numbers of observations are stated as n values and, unless indicated otherwise, refer to the number of neurones from which an observation was made. Significance of differences was determined using the Mann–Whitney two-tailed test unless stated otherwise. Correlation between variables was determined using Spearman rank order correlation.

For cross-correlation analysis voltage recordings of greater than 10 min duration containing spontaneous action potential firing were converted off-line into event lists using Spike 2 software. Events were triggered when the action potential rising phase crossed a threshold set to approximately half the maximal action potential amplitude. Cross-correlograms were constructed with a bin width of 1 ms.

Neuronal input resistance and coupling coefficients were determined from the membrane potential responses to injection of a series of current steps into either neurone. Neurones were described as presynaptic when they were the cell in which a membrane potential change was initiated, either by injection of current or following action potential firing and were termed postsynaptic when they responded to a membrane potential change in an adjoining neurone. In this manner each neurone in a pair could be described as either pre- or postsynaptic. Input resistance was calculated from the slope, around the resting membrane potential, of the relationship between injected current and the corresponding change in presynaptic membrane potential. The coupling coefficient was determined from the ratio of presynaptic to postsynaptic membrane potential changes.

The junctional conductance (g_j) was estimated from experimentally measured input resistances and coupling coefficients using a model in which each neurone was represented by a single compartment joined by a resistor representing the electrical synapse (Bennett, 1966, 1977):

$$g_{j12} = R_1 k_{12}/((R_1 R_2) - (R_1 k_{12})^2),$$

where R_1 and R_2 are the input resistances of the pre- and post-synaptic neurones, respectively, and k_{12} is the coupling coefficient between the pre- and postsynaptic neurone.

To examine spike-evoked postsynaptic potentials, 5–60 presynaptic action potentials and the corresponding postsynaptic membrane potential responses were captured to computer. Each trace was examined visually and traces in which spontaneous synaptic activity occurred during the postsynaptic response, or in which

action potentials fired coincidentally in adjoining neurones, as indicated by large variability in the duration of the presynaptic action potential afterhyperpolarisation (AHP), were rejected from the analysis. Those connections for which a monosynaptic response could be clearly identified were selected for analysis. The peak amplitude of the depolarising and hyperpolarising responses was measured for each response with respect to a baseline period of duration 2–4 ms immediately before the presynaptic spike. Baseline noise was estimated from the variability in membrane potential at corresponding time periods preceding the postsynaptic response (see Mason *et al.* 1991).

Presynaptic action potential waveforms were transformed digitally to fit the postsynaptic waveform using a model circuit containing resistors representing the junctional conductance and postsynaptic input resistance and a capacitor representing the postsynaptic membrane capacitance (run as a program module within Axograph3). Values of the parameters which gave the best fit to the postsynaptic response were determined iteratively using a least-squares fitting procedure. By constraining the value of the post-synaptic input resistance to the experimentally measured value, the fitting procedure also allowed estimation of the junctional conductance.

RESULTS

Simultaneous whole-cell current-clamp recordings were made from over 200 pairs of SPNs. Electrotonic coupling was demonstrated between 21 pairs of SPNs by induction of a membrane polarisation in one cell following current injection into the other cell. Current injection into either cell caused membrane polarisation in both cells, and therefore either cell could be regarded as pre- or postsynaptic depending upon which was driving the membrane potential change. Neurones in coupled pairs had resting membrane potentials of -61 ± 1 mV and input resistances of 213 ± 19 MΩ. Patterns of spontaneous activity were similar to those described previously (Spanswick & Logan, 1990; Logan *et al.* 1996). Similar activity was observed in both neurones from 20 pairs: cells were classified as silent if they did not fire spontaneous action potentials or demonstrate subthreshold rhythmic activity ($n = 9$ pairs) and oscillating if they displayed rhythmic subthreshold membrane potential oscillations with or without spontaneous action potential firing ($n = 11$ pairs). In the remaining pair, one neurone was
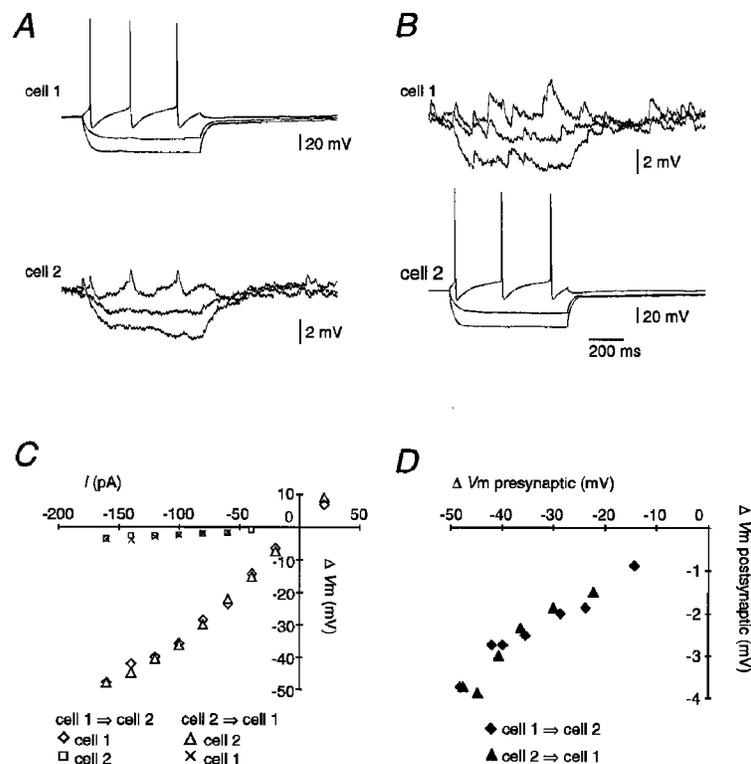

Figure 1. Symmetrical voltage-independent electrotonic coupling between SPNs

A, simultaneous recordings from two electrotonically coupled SPNs, demonstrating conduction of membrane potential changes from cell 1 to cell 2. A series of rectangular-wave current steps (amplitude, −160, −80 and 40 pA; duration, 800 ms) injected into cell 1 elicited corresponding membrane potential responses in both neurones. *B*, recordings from the same pair of neurones as in *A* showing conduction of membrane potential changes from cell 2 to cell 1, following injection of current steps (amplitude, −160, −80 and 40 pA; duration, 800 ms) into cell 2. Transient depolarisations in cell 1 are spontaneous chemically mediated excitatory postsynaptic potentials. *C*, plot of the relationship between the injected current and the steady-state membrane potential responses of each neurone. *D*, plot of the relationship between pre- and postsynaptic changes in membrane potential.

silent and the other fired spontaneous action potentials without any underlying subthreshold rhythmic activity.

Steady-state coupling

The relationship between pre- and postsynaptic changes in membrane potential was determined from the response of both neurones to injection of current steps into either neurone (Figs 1 and 2). The amplitude of the membrane potential change in the postsynaptic cell was smaller and the time course slower than in the presynaptic cell (Figs 1 and 2). The relationship between the amplitude of the pre- and postsynaptic membrane potential changes appeared linear (Figs 1D and 2D), indicating that the strength of coupling was independent of the transjunctional potential over the range of potentials examined.

Coupling coefficients, defined as the ratio of the post-synaptic to presynaptic potential change (Bennett, 1966), ranged from 0·02 to 0·48 (mean, 0·18 ± 0·02; $n = 40$). Pairs of neurones between which monosynaptic connections were

demonstrated (see below) had coupling coefficients of 0·04–0·46 compared with 0·02–0·42 for the remaining connections ($P = 0·64$). Junctional conductance was estimated using a simple model in which each neurone was considered as a single compartment coupled by a resistance representing the electrical synapse (Bennett, 1966, 1977; see Methods). Estimates of junctional conductance for confirmed monosynaptic connections ranged from 0·2 to 2·9 nS (mean, 1 ± 0·2 nS; $n = 14$; Fig. 3B).

Comparison of the coupling coefficient in either direction, showed that between some pairs of neurones, including those between which monosynaptic connections were demonstrated, membrane potential changes were transferred more efficiently in one direction (Figs 2 and 3A). This apparent rectification was quantified using the ratio of the larger to the smaller coupling coefficient for each connection (mean, 1·7 ± 0·2; $n = 20$ pairs). The mean ratio was skewed towards positive values by four pairs of neurones which
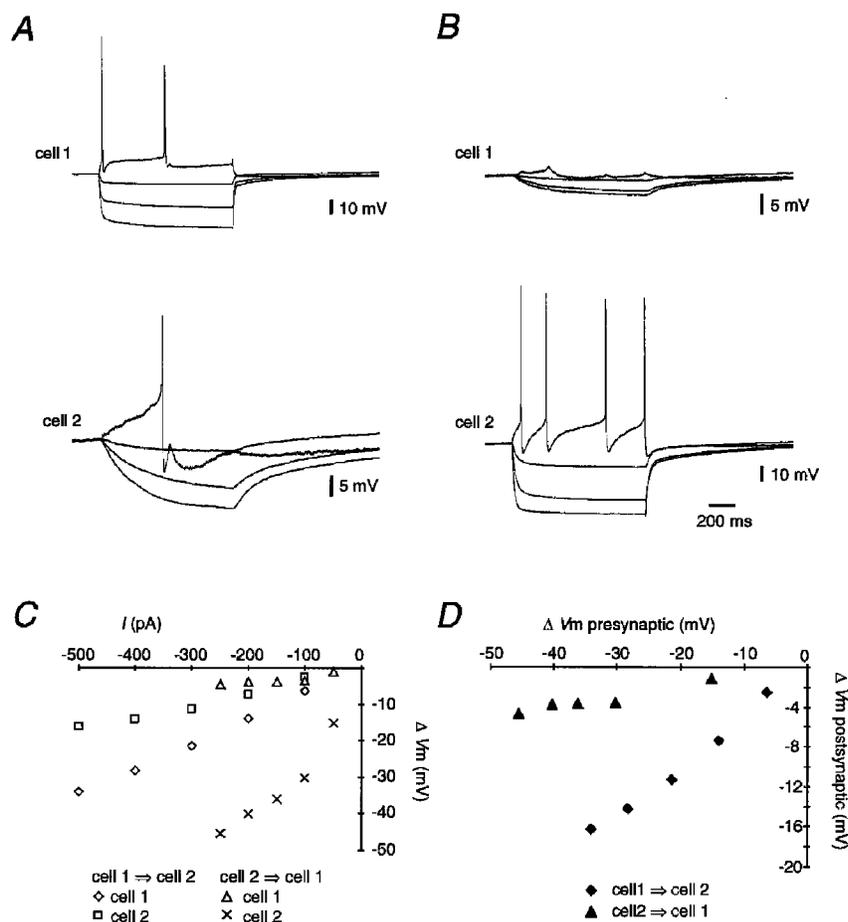

Figure 2. Asymmetrical electrotonic coupling between SPNs

A, simultaneous recordings from two SPNs in which membrane potential changes were transferred preferentially in the direction from cell 1 to cell 2. Rectangular-wave current steps (amplitude, −500, −300, −100 and 200 pA; duration, 1000 ms) were injected into cell 1 and corresponding membrane potential responses of both neurones recorded. *B*, weaker coupling was observed in the direction from cell 2 to cell 1. Membrane potential responses of both neurones are shown following injection of current steps (−250, −150, −50 and 50 pA; duration, 1000 ms) into cell 2. *C*, plot of the relationship between injected current and steady-state membrane potential responses of each neurone. *D*, plot of the relationship between pre- and postsynaptic changes in membrane potential.

appeared to have strongly rectifying connections (ratio, 2·2–4·8; e.g. Fig. 2), whereas in 12 pairs the ratio was less than 1·5 (e.g. Fig. 1). At giant motor synapses of the crayfish, rectification is due to asymmetry of the junctional conductances (Jaslove & Brink, 1986). Comparison of conductance estimates for coupling in each direction, shown in Fig. 3*B*, demonstrated that the underlying conductance was similar in either direction, indicating that such a mechanism does not account for the apparent rectification between SPNs. Preferential transmission of membrane potential changes in one direction can also be caused by differences between the input resistance of coupled neurones (Bennett, 1966). In three pairs of SPNs with a ratio of the larger to the smaller coupling coefficient greater than 2 (mean, 3·4 ± 0·8), the corresponding ratios for the post-synaptic input resistance and junctional conductance were 2·8 ± 0·8 and 1·2 ± 0·2, respectively, indicating that this is also the case for electrical synapses between SPNs. Comparison of the coupling coefficient ratio with the corresponding ratio of input resistances for all pairs of neurones, also suggested that the apparent rectification occurred between neurones with different input resistances and that the larger coupling coefficient was associated with coupling from the lower input resistance to the higher input resistance neurone (Figs 2 and 3*C*).

Conduction of action potentials

Postsynaptic responses to action potentials evoked by injection of positive current into either neurone were examined (Fig. 4). In some coupled and non-coupled neurones a fast postsynaptic depolarising transient (amplitude usually < 0·1 mV) occurred simultaneously with the rising phase of the presynaptic spike. This transient was not considered further as it could still be observed following removal of the electrode from the postsynaptic cell and was thus attributed to extracellular field effects (Jefferys, 1995). Electrotonically mediated postsynaptic potentials (ePSPs) were conducted bidirectionally and had waveforms resembling single spontaneous subthreshold membrane potential oscillations, consisting of an initial depolarising component followed by a slower hyperpolarising component (Fig. 4). The ePSPs were not observed following withdrawal of the postsynaptic electrode and therefore were not due to generation of extracellular field potentials.

In nine pairs of neurones ePSPs were characterised by an absence of failures, constant latency and insensitivity of the initial depolarising component to changes in the frequency of the presynaptic action potentials (e.g. Figs 4 and 6), indicating that they were not mediated polysynaptically via spike firing in an intermediate neurone. In these neurones,

Figure 3. Pooled data for steady-state properties of electrotonic coupling
A, logarithmic plot comparing coupling coefficients for conduction in each direction across electrical synapses for confirmed monosynaptic connections (O) and the remaining coupled pairs of neurones (other connections, □). Coefficients for coupling from cell 1 to cell 2 are plotted on the ordinate (*k*1−2) and for coupling from cell 2 to cell 1 on the abscissa (*k*2−1). The diagonal line corresponds to symmetrical coupling (*k*1−2 is the same as *k*2−1) and has a slope of 1. *B*, logarithmic plot comparing coupling conductances (*g*) in each direction for confirmed monosynaptic (O) and other connections (□). The notation for the direction of coupling is the same as in *A*. The diagonal line represents the values expected when the underlying conductance is similar in either direction and has a slope 1. *C*, relationship between apparent rectification and input resistance. The coupling coefficient ratio for each connection is the ratio of the higher to the lower coupling coefficient (K ratio). The input resistance ratio for each pair is the ratio of the input resistance of the postsynaptic cell to the presynaptic cell for coupling in the direction of the larger coupling coefficient. The horizontal line represents points expected for pairs of neurones with similar coupling coefficients in either direction. The vertical line corresponds to expected points for pairs of neurones with identical input resistances. The diagonal line has slope 1 and corresponds to points expected for pairs of neurones connected by a symmetrical conductance.
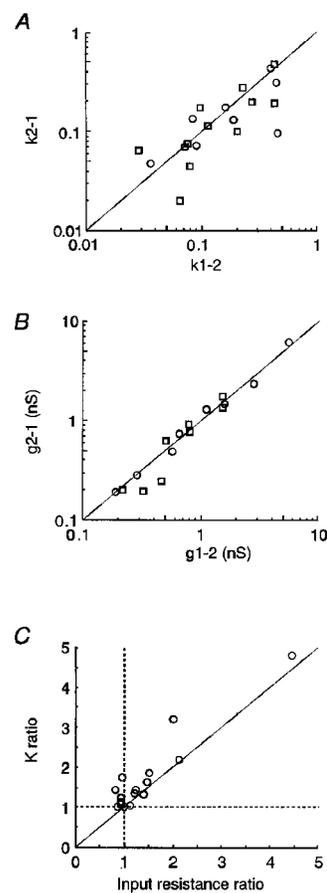
for which the coupling was attributed to a monosynaptic connection, the amplitude of the initial depolarising component was in the range 0·3–4·7 mV (mean, 1·2 ± 0·2 mV), had a mean 10–90% rise time of 4·2 ± 0·6 ms and a half-duration of 16·0 ± 1·8 ms. No significant correlation was found between the amplitude and 10–90% rise time ($P > 0·1$), indicating that the amplitude was not due primarily to the electrotonic distance of the synapses from the soma. The variation in the amplitude of the depolarising component of the ePSPs was not significantly different from that of the background noise ($P > 0·1$, F test, see Mason *et al.* 1991), demonstrating that the synapses reliably mediate reciprocal transfer of information between neurones. The 10–90% rise time and half-duration of the ePSPs were positively correlated with the junctional conductance ($r = 0·54$, $P = 0·05$ and $r = 0·8$, $P = 0·0006$, respectively), but not with the coupling coefficient or postsynaptic input resistance ($P > 0·1$). No significant correlation was found between the amplitude of the depolarising component and any of the steady-state properties ($P > 0·1$).

In 15 of the 18 monosynaptically connected neurones the initial depolarising component of the ePSP was followed by a hyperpolarisation. At presynaptic spike frequencies below 3 Hz, the hyperpolarising component had amplitudes in the range 0·6–9·0 mV (mean, 2·1 ± 0·6 mV), and had mean

half-duration of 182 ± 27 ms. The amplitude of the hyperpolarisation was positively correlated with that of the corresponding depolarising component ($r = 0·60$, $P = 0·02$), but did not show any significant correlation with the coupling coefficient, junctional conductance, or postsynaptic input resistance ($P > 0·1$).

In order to determine if electrotonic conduction of a presynaptic spike across an electrical synapse to a post-synaptic neurone could account for the complex biphasic waveform of the ePSP, presynaptic action potential waveforms were digitised and used as the input waveform to a model circuit composed of a junctional resistance coupled to postsynaptic resistance and capacitance (see Methods). The values of the circuit components which gave the best fit to the experimentally measured postsynaptic waveform were determined iteratively. For monosynaptic coupling in either direction, the waveform of the transformed presynaptic action potential resembled that of the postsynaptic response, consisting of an initial depolarisation followed by a more prolonged hyperpolarisation ($n = 14$; Fig. 5*A*). Transformation of presynaptic membrane potential responses to negative current steps also gave waveforms closely resembling the corresponding postsynaptic response (data not shown). The amplitude and time course of the transformed action potential waveforms were similar to
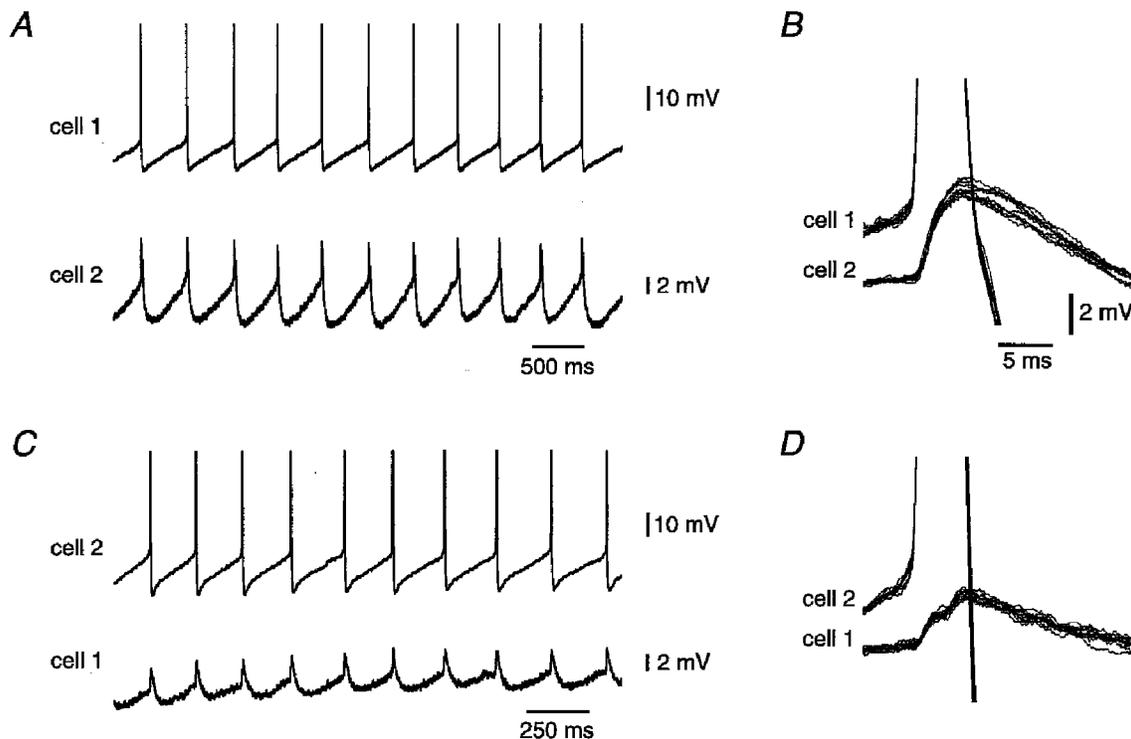

Figure 4. Conduction of action potential waveforms across electrical synapses

A, action potentials fired during injection of constant depolarising current into cell 1 (upper trace) elicited postsynaptic potentials in cell 2 (lower trace). *B*, ten superimposed consecutive action potentials evoked in cell 1 and the corresponding ePSPs recorded from cell 2, demonstrating the lack of variation in the amplitude and waveform of the ePSP. *C*, action potentials were conducted bidirectionally, as shown by ePSPs observed in cell 1 (lower trace) in response to action potentials elicited by injection of constant depolarising current into cell 2 (upper trace). *D*, ten superimposed consecutive action potentials evoked in cell 2 and the corresponding ePSPs recorded from cell 1.

those of experimentally recorded ePSPs: the depolarising component had an amplitude of $0·6 \pm 0·1$ mV, a 10–90% rise time of $3·1 \pm 0·1$ ms and a half-duration of $13 \pm 3·1$ ms; the hyperpolarising component had an amplitude of $1·6 \pm 0·4$ mV and a half-duration of 207 ± 28 ms, thus indicating that electrical synapses between two neurones can account for the experimentally observed ePSPs. We next used the model to provide an independent estimate of the junctional conductance. By constraining the postsynaptic input resistance used in the fitting procedure to the experimentally measured value, the junctional conductance was estimated to be $1 \pm 0·2$ nS ($n = 10$). The resulting waveforms were identical to those obtained from the unconstrained fits and the conductance estimates were not significantly different from those obtained more directly from the steady-state coupling properties ($P > 0·1$). Thus, conduction of action potentials across electrical synaptic connections with conductance of approximately 1 nS can account for the waveform of ePSPs recorded from SPNs.

More detailed examination of the relationship between the pre- and postsynaptic membrane potential waveforms suggested that connections between SPNs behave as low-pass filters: high frequency components, such as action potentials, were strongly attenuated, slower events such as the action potential afterhyperpolarisation (AHP) were less attenuated and steady-state membrane potential changes were the least attenuated (Figs 4 and 5). Furthermore, the dependence of the postsynaptic response on the frequency of the presynaptic waveform would be expected, from the two compartment model, to resemble the frequency response

properties of a low-pass filter (Bennett, 1977; Fig. 5*B*). The corner frequencies (for attenuation to $1/\sqrt{2}$ of the steady-state response) of the equivalent low-pass filters, estimated by analysis of the model using component values obtained from the constrained fits of the transformed presynaptic to postsynaptic waveforms, ranged from $0·2$ to $4·8$ Hz (Fig. 5*B*). This corresponds to wavelengths of 208–5000 ms, which are similar to the duration of the action potential AHP. Therefore, we hypothesised that the hyperpolarising component of the ePSP would be particularly sensitive to changes in the duration of the presynaptic action potential AHP. When the frequency of presynaptic action potential firing was increased, from $2·4 \pm 0·3$ to $11·2 \pm 3·7$ Hz, the half-duration of the presynaptic AHP was reduced by $66·2 \pm 3·8\%$ (from 143 ± 39 to 54 ± 20 ms; $n = 6$). The increased firing rate caused a corresponding reduction of $68·4 \pm 7·1\%$ in the amplitude of the hyperpolarising component of the ePSP (from $2·8 \pm 1·3$ to $1·1 \pm 0·6$ mV), but had little effect on the amplitude of the depolarising component of the ePSP (reduction of $8·6 \pm 4·9\%$, from $1·8 \pm 0·6$ to $1·6 \pm 0·6$ mV; Fig. 6). The amplitude of the presynaptic AHP was reduced by $23·9 \pm 3·6\%$ (from $23·4 \pm 1·8$ to $18·0 \pm 1·7$ mV) and could therefore only account for a small proportion of the observed attenuation in the hyperpolarising component of the ePSP, consistent with the attenuation being primarily due to the filtering properties of the synapses. Furthermore, transformation of relatively high-frequency presynaptic action potentials, using the model described above with component values obtained from action potentials occurring at low frequencies, gave waveforms similar to the recorded postsynaptic waveform

Figure 5. Low-pass filtering of presynaptic action potentials

A, the presynaptic action potential shown in *a* was transformed using a model circuit representing the junctional conductance and postsynaptic membrane resistance and capacitance (see Methods) to give the waveform shown in *b*. The recorded postsynaptic response to the presynaptic action potential is shown in *c*. The transformed (dashed line) and experimentally recorded waveforms (thick line) are superimposed in *d*, demonstrating that the simple model containing a small conductance electrical synapse (0·5 nS in this case) can account for the dynamic properties of the observed electrotonic coupling. *B*, the two compartment model used to examine the electrical synaptic connections behaves in a similar manner to a low-pass filter. The graph shows the predicted relationship between the frequency of presynaptic membrane potential waveforms and their attenuation, expressed as ratio of the amplitude of the pre- to the corresponding postsynaptic waveforms, obtained using the model of the data shown in *A*.
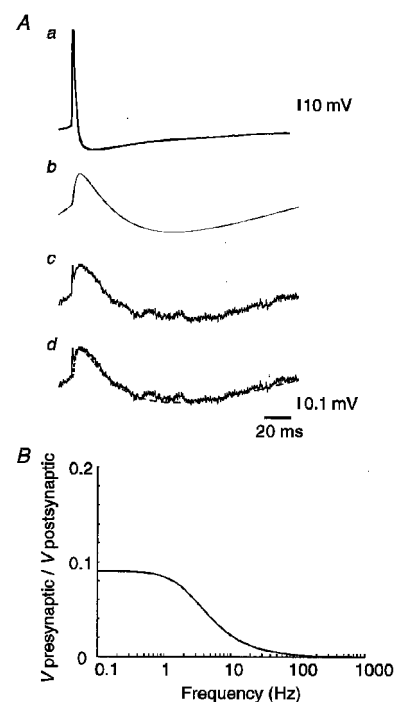
(Fig. 6), also indicating that modulation of the ePSP waveform was due to the intrinsic frequency dependence of communication across the synapses, rather than changes in the junctional conductance or neuronal membrane properties.

Action potential synchronisation

Spontaneous subthreshold membrane potential oscillations resembled repetitive ePSPs and were synchronised between electrotonically coupled neurones (Fig. 7). Cross-correlation analysis was used to examine synchronisation of spike firing between electrotonically coupled neurones demonstrating spontaneous membrane potential oscillations. Cross-correlograms had peaks corresponding to a delay of 15 ± 4 ms between action potential firing in each neurone, but otherwise had few events within a ± 300 ms time window ($n = 6$ pairs; Fig. 7A). Spread of events was observed around the peaks indicating variability in the delay. However, the delay between spike firing in coupled cells was small with respect to their firing rates (< 1 Hz), indicating that action potentials were highly synchronised.

Repetitive ePSPs resembling spontaneous membrane potential oscillations were observed in silent neurones when an adjoining electrotonically coupled neurone was driven

to fire action potentials by injection of positive current (Fig. 7B). When the depolarising component of the ePSP reached threshold single action potentials were fired ($n = 4$). Delays between pre- and postsynaptic spikes were $11 \cdot 1 \pm 3 \cdot 5$ ms ($n = 4$), compared with interspike intervals of greater than 200 ms, indicating that action potentials fired by a single presynaptic neurone are sufficient to synchronise activity in postsynaptic neurones via electrical synapses.

DISCUSSION

The data described characterise bidirectional, voltage-independent electrical synapses with non-rectifying conductances of approximately 1 nS capable of synchronising SPNs. Presynaptic action potentials elicited biphasic postsynaptic potentials consisting of an initial 0·3–4·7 mV depolarisation, followed by a slower 0·6–9 mV hyperpolarisation. Postsynaptic potentials elicited by action potential firing in a single neurone were sufficient to drive synchronous activity in adjoining neurones. Waveforms similar to the postsynaptic potential were obtained by transformation of the presynaptic action potential using an equivalent circuit model of the electrical synapse and
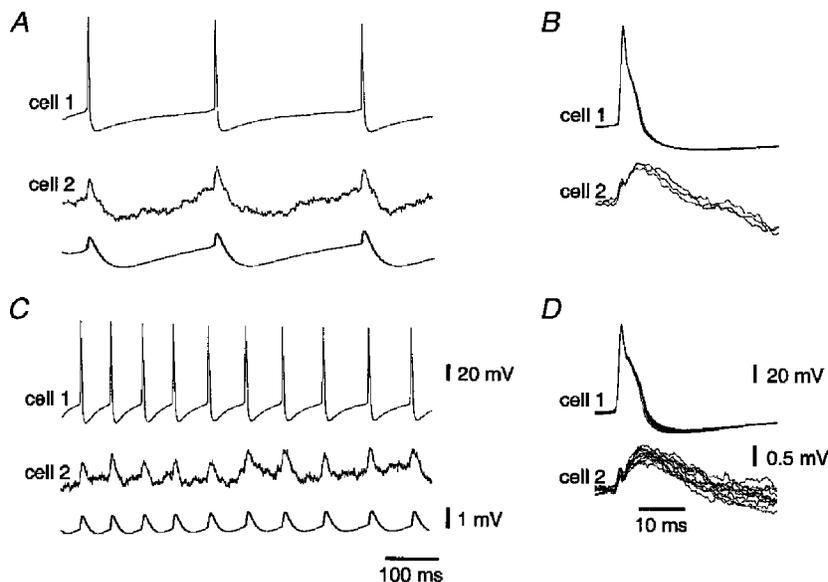

Figure 6. Frequency dependence of action potential conduction

A, action potentials, firing at a frequency of 2·6 Hz, were evoked in cell 1 by injection of constant positive current (top trace). The corresponding postsynaptic potentials recorded from cell 2 are shown in the middle trace. The lower trace shows the waveform obtained by transformation of the presynaptic action potential waveforms to fit the corresponding postsynaptic responses using the two compartment model. B, super-imposition of the three consecutive action potentials and postsynaptic responses shown in A, demonstrating the constant latency and waveform of the depolarising component of the ePSP. C, recordings from the same pair of cells as in A and B, showing injection of increased positive current into cell 1 induced action potentials firing at a frequency of 12·2 Hz (upper trace) and corresponding postsynaptic potentials in cell 2 (middle trace). The hyperpolarising component of the ePSP was attenuated compared to ePSPs evoked at the lower frequency shown in A. The lower trace shows the waveform obtained by transformation of the presynaptic action potential waveforms using the two compartment model with parameters obtained from the transformation in A, thus demonstrating that the attenuation of the hyperpolarising component of the ePSP does not require changes in the junctional conductance or postsynaptic membrane properties. D, ten superimposed consecutive action potentials and postsynaptic responses from C demonstrating constant latency and waveform.

postsynaptic neurone, supporting the conclusion that the recorded ePSPs could be accounted for by electrical synaptic transmission with similar coupling conductances to those measured experimentally.

Classification of connections as monosynaptic was based on the properties of ePSPs evoked between pairs of neurones. Criteria based on constant latency and waveform of the depolarising component of the ePSP were sufficient to reject the possibility that ePSPs were mediated polysynaptically via initiation of action potential firing in an adjoining neurone. A second possibility is that ePSPs were mediated polysynaptically through passive conduction via an intermediate neurone. Compared with a monosynaptic pathway, this would involve a greater electrotonic distance between the recorded neurones and therefore increased attenuation of their amplitude and slowing of their kinetics (Spruston *et al.* 1992). A number of observations indicate that the ePSPs characterised were not mediated by such a pathway. The

rise times of the depolarising components of ePSPs were similar to or faster than the fastest chemical excitatory inputs to SPNs, evoked by stimulation of the contra- or ipsilateral lateral funiculi and likely to synapse on or near the soma of SPNs (see Morrison *et al.* 1989; Krupp & Feltz, 1995; Spanswick *et al.* 1998), suggesting that the ePSPs arise at or close to the soma. If the ePSPs were conducted passively through an intermediate neurone, occasional recordings of spontaneous or antidromically evoked electrotonically mediated membrane potential oscillations with considerably larger amplitudes and faster kinetics than ePSPs between pairs of SPNs would be expected, but have not been observed (cf. Spanswick & Logan, 1990; Logan *et al.* 1996). The ePSPs characterised were also unlikely to result from a mixture of monosynaptic and passively conducted polysynaptic inputs, as there was no significant relationship between their amplitude and rise times, which would otherwise be expected from the resulting variability in the
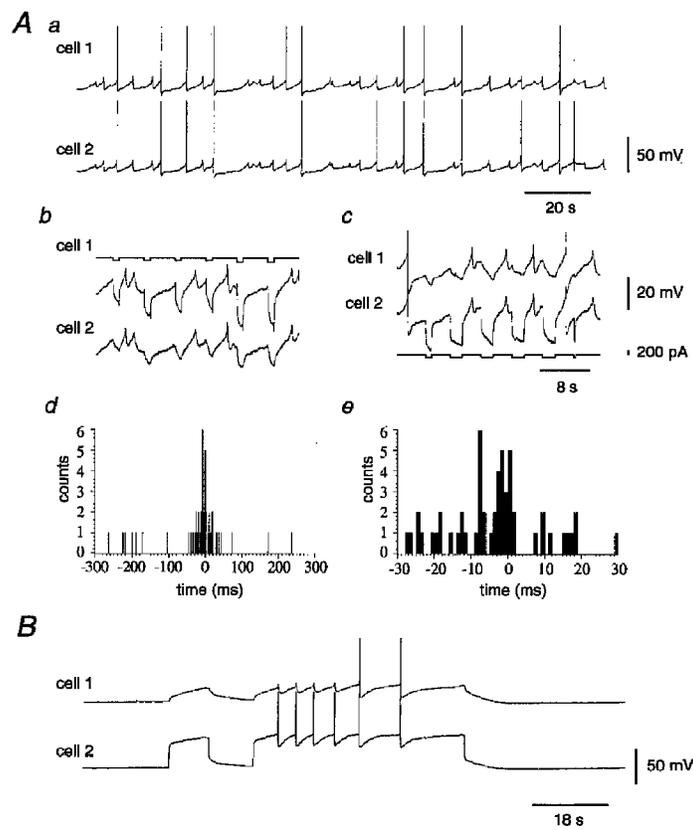

Figure 7. Synchronisation of action potential firing between electrotonically coupled SPNs

A, synchronous action potential firing and subthreshold membrane potential oscillations recorded from two electrotonically coupled SPNs in a spinal cord slice. Continuous membrane potential recordings made simultaneously from two SPNs demonstrate synchronisation of neuronal activity (*a*) and polarisation of both neurones following injection of current into either neurone, indicating electrotonic coupling from cell 1 to cell 2 (*b*) and from cell 2 to cell 1 (*c*). Upper trace in *b* and lower trace in *c* correspond to current injected into cell 1 and cell 2, respectively. Cross-correlation of action potential firing between the cells in *a–c* is shown for a ± 300 ms time window in *d* and for a ± 30 ms time window in *e*. Data for the cross-correlation was obtained from a continuous recording period of 26 min. Bin width is 1 ms. *B*, action potentials drive membrane potential oscillations and synchronous action potential firing in adjoining electrotonically coupled neurones. Injection of positive current into cell 2 caused depolarisation of both cells. When polarisation of cell 2 was suprathreshold (second step), membrane potential oscillations were observed in cell 1 which on reaching threshold evoked synchronous action potentials.

lengths of their conduction pathways. Finally, the waveform of the ePSPs could be accounted for by the model containing two monosynaptically coupled neurones. We therefore conclude that the ePSPs characterised were mediated by monosynaptic connections between the recorded neurones.

The conductance of electrical synapses between SPNs was estimated to be approximately 1 nS. The reliability of these estimates depends upon the assumption that little attenuation of steady-state membrane potential changes occurs between the recording electrode and the site of coupling. This is supported by equivalent cylinder models which suggest that between somatic and proximal dendritic regions, only small attenuation of steady-state currents occurs (Spruston *et al.* 1992) and by similar estimates of junctional conductance after experimentally induced increases in input resistance, which would be expected to reduce attenuation of distal electrical events (M. F. Nolan, S. D. Logan & D. Spanswick, unpublished observations). Furthermore, similar conductance values were obtained by fitting transformed presynaptic to postsynaptic waveforms, demonstrating that these values can account for dynamic as well as steady-state communication between coupled cells. Our estimates are also consistent with the suggested threshold conductance of 2 nS for detecting Lucifer Yellow dye coupling (Dermietzel, 1996), which is rarely observed following recordings from electrotonically coupled SPNs (Logan *et al.* 1996). A junctional conductance of 1 nS could be conducted by less than 5 up to approximately 500 connexons, depending on their single channel conductance and open probability (Zampiglui *et al.* 1985; Burt & Spray, 1988; Chanson *et al.* 1993; Bukauskas *et al.* 1995; Spray, 1996). Hence, relatively few gap junction channels may be sufficient for coupling of neurones.

The efficacy with which membrane potential changes were communicated between neurones depends on the junctional conductance and the postsynaptic input resistance (Bennett, 1966, 1977). The absence of voltage dependence for the coupling coefficient or junctional conductance contrasts with steep voltage dependence of gap junctions between some non-neuronal cells (e.g. Chanson *et al.* 1993), and may reflect differences in the expression of connexins forming the electrical synapses. The relatively wide range of coupling coefficients for monosynaptically coupled neurones may reflect functional differences between populations of neurones with different postsynaptic targets or differences in the strength of connections within networks of SPNs projecting to the same target. The existence of asymmetrical coupling between some pairs of SPNs suggests the latter alternative may occur. This apparent rectification was accounted for by differences between the input resistance of the neurones rather than true rectification of the junctional conductance (see Bennett, 1966, 1977). Thus, polarisation of a relatively high input resistance neurone had a small effect on the membrane potential of a lower input resistance neurone, whereas polarisation of the lower input resistance neurone caused relatively large changes in the membrane potential of

the higher input resistance neurone. Functionally, this may enable one neurone to dominate the activity of other neurones, but without itself being influenced by activity in these neurones.

Biphasic ePSPs similar to those observed between SPNs have been shown in the inferior olive, supraoptic nucleus and nucleus ambiguus (Llinás & Yarom, 1981; Zhang & Hatton, 1988; Rekling & Feldman, 1997), whereas in hippocampal CA3 pyramidal cells ePSPs appear as monophasic depolarisations (MacVicar & Dudek, 1981). Antidromic activation of SPNs evokes ePSPs of similar waveform, which are insensitive to high Mg^{2+}/low Ca^{2+} ACSF indicating that they are not mediated by chemical transmission (Logan *et al.* 1996); however, this method of stimulation activates an unknown number of presynaptic neurones hindering characterisation of the ePSP. The waveform of the ePSPs recorded from SPNs in response to single presynaptic action potentials was determined by the presynaptic membrane potential waveform in conjunction with the resistive and capacitative properties of the synapse and postsynaptic membrane which behaved as a low-pass filter. However, factors such as active conductances and cable properties of postsynaptic neurones may also influence the waveform of ePSPs. Comparison of ePSPs evoked at different presynaptic spike frequencies demonstrated a novel mechanism for frequency-dependent modulation of the postsynaptic response at electrical synapses. The depolarising component of the ePSP was relatively insensitive to frequency, whereas the hyperpolarising component was attenuated by increasing the frequency of presynaptic spikes. This effect was due to increased filtering of the reduced duration presynaptic action potential and demonstrates the importance of the intrinsic frequency dependence of electrotonic coupling between neurones. Functionally, frequency-dependent modulation of postsynaptic responses may allow the inhibitory actions of the hyperpolarising component of the ePSP to be overcome by stimuli which drive neurones to fire at sufficiently high frequencies, adding further to the possible computation roles played by electrical synapses (Marder, 1998).

In a previous study we demonstrated that action potential firing can be synchronised between electrotonically coupled SPNs (Logan *et al.* 1996). The data described here demonstrate that action potential firing in a single presynaptic SPN can drive ePSPs of sufficient amplitude to mediate synchronisation of action potential firing between neurones. The depolarising component of the ePSP increases the probability of action potential firing immediately following the presynaptic spike and the subsequent slow hyperpolarising component reduces the probability of firing during the period in which the presynaptic cell is silent. The continuum of ePSP amplitudes extended from 0·4 to 4·7 mV and it is likely that synchronisation of cells which receive smaller amplitude ePSPs may involve summation of ePSPs from multiple presynaptic neurones. Examination of synchronous firing on a millisecond time scale revealed

variable delays between spikes, reflecting the relatively slow kinetics of the ePSPs. However, the delays were small with respect to the firing rates of SPNs (McAllen & Malpas, 1997; Malpas, 1998), and were shorter than the duration of excitatory postsynaptic potentials from preganglionic to postganglionic neurones (e.g. Blackman & Purves, 1969; McLachlan *et al.* 1997). Hence, the degree of synchronisation should be sufficient to contribute to the generation of coherent sympathetic rhythms, and for spatial summation of convergent inputs onto the same postganglionic neurone.

In conclusion, these data demonstrate that central electrical synapses with conductance of approximately 1 nS and thus composed of relatively few gap junction channels, can sustain steady-state coupling with coefficients greater than 0·1 and are capable of synchronising action potential firing between neurones. Synchronisation of activity between SPNs appears to involve reliable, reciprocal communication of sub- and suprathreshold neuronal activity by electrical synapses, with firing of action potentials by one or a small number of presynaptic neurones being sufficient to drive synchronisation of activity between adjoining neurones. The low-pass filter characteristics of these synapses suggest a cellular mechanism which may promote expression of relatively low frequency synchronised sympathetic rhythms, for example those recorded from the caudal ventral artery of the tail (Johnson & Gilbey, 1996; Chang *et al.* 1999).

BENNETT, M. V. L. (1966). Physiology of electrotonic junctions. *Annals of the New York Academy of Sciences* **137**, 509–539.

BENNETT, M. V. L. (1977). Electrical transmission: a functional analysis and comparison to chemical transmission. In *Handbook of Physiology*, vol. 1, *The Nervous System*, ed. KANDEL, E. R., pp. 357–416. Williams and Wilkins, Baltimore.

BENNETT, M. V. L. (1997). Gap junctions as electrical synapses. *Journal of Neurocytology* **26**, 349–366.

BLACKMAN, J. G. & PURVES, R. D. (1969). Intracellular recordings from ganglia of the thoracic sympathetic chain of the guinea-pig. *Journal of Physiology* **203**, 173–198.

BUKAUSKAS, F. F., ELFGANG, C., WILLECKE, K. & WEINGART, R. (1995). Biophysical properties of gap junction channels formed by mouse connexin 40 in induced pairs of transfected HeLa cells. *Biophysical Journal* **68**, 2289–2298.

BURT, J. M. & SPRAY, D. C. (1988). Single-channel events and gating behaviour of the cardiac gap junction channel. *Proceedings of the National Academy of Sciences of the USA* **85**, 3431–3434.

CHANG, H.-S., STARAS, K., SMITH, J. E. & GILBEY, M. P. (1999). Sympathetic neuronal oscillators are capable of dynamic synchronization. *Journal of Neuroscience* **19**, 3183–3197.

CHANSON, M., CHANDROSS, K. J., ROOK, M. B., KESSLER, J. A. & SPRAY, D. C. (1993). Gating characteristics of a steeply voltage-dependent gap junction channel in rat Schwann cells. *Journal of General Physiology* **102**, 925–946.

DERMIETZEL, R. (1996). Molecular diversity and plasticity of gap junctions in the nervous system. In *Gap Junctions in the Nervous System*, ed. SPRAY, D. C. & DERMIETZEL, R., pp. 13–38. Springer-Verlag, Heidelberg.

DRAGUHN, A., TRAUB, R. D., SCHMITZ, D. & JEFFERYS, J. G. R. (1998). Electrical coupling underlies high-frequency oscillations in the hippocampus *in vitro. Nature* **349**, 189–192.

GEBBER, G. L. (1980). Central oscillators responsible for sympathetic discharge. *American Journal of Physiology* **239**, H143–155.

JANIG, W. & McLACHLAN, E. (1992). Characteristics of function specific pathways in the sympathetic nervous system. *Trends in Neurosciences* **15**, 475–481.

JASLOVE, S. W. & BRINK, P. R. (1986). The mechanism of rectification at the electrotonic giant synapse of the crayfish. *Nature* **323**, 63–65.

JEFFERYS, J. G. R. (1995). Nonsynaptic modulation of neuronal activity in the brain: electric currents and extracellular ions. *Physiological Reviews* **75**, 689–723.

JOHNSON, C. D. & GILBEY, M. P. (1996). On the dominant rhythm in the discharges of single postganglionic sympathetic neurones innervating the rat tail artery. *Journal of Physiology* **497**, 241–259.

KRUPP, J. & FELTZ, P. (1995). Excitatory postsynaptic currents and glutamate receptors in neonatal rat sympathetic preganglionic neurons *in vitro. Journal of Neurophysiology* **73**, 1503–1512.

LLINÁS, R. (1985). Electrotonic transmission in the mammalian central nervous system. In *Gap Junctions,* ed. BENNETT, M. V. L. & SPRAY, D. C., pp. 325–353. Cold Spring Harbor Laboratory, New York.

LLINÁS, R. & YAROM, Y. (1981). Electrophysiology of mammalian inferior olive neurones *in vitro.* Different types of voltage-dependent ionic conductances. *Journal of Physiology* **315**, 549–567.

LOGAN, S. D., PICKERING, A. E., GIBSON, I. C., NOLAN, M. F. & SPANSWICK, D. (1996). Electrotonic coupling between rat sympathetic preganglionic neurones *in vitro. Journal of Physiology* **495**, 491–502.

McALLEN, R. M. & MALPAS, S. C. (1997). Sympathetic activity: characteristics and significance. *Clinical and Experimental Pharmacology and Physiology* **24**, 791–799.

McLACHLAN, E. M., DAVIES, P. J., HABLER, H.-J. & JAMIESON, J. (1997). On-going and reflex synaptic events in rat superior cervical ganglion cells. *Journal of Physiology* **501**, 165–182.

MacVICAR, B. A. & DUDEK, F. E. (1981). Electrotonic coupling between pyramidal cells: a direct demonstration in rat hippocampal slices. *Science* **213**, 782–785.

MALPAS, S. C. (1998). The rhythmicity of sympathetic nerve activity. *Progress in Neurobiology* **56**, 65–96.

MARDER, E. (1998). Electrical synapses: beyond speed and synchrony to computation. *Current Biology* **8**, R795–797.

MASON, A., NICOLL, A. & STRATFORD, K. (1991). Synaptic transmission between individual pyramidal neurons of the rat visual cortex *in vitro. Journal of Neuroscience* **11**, 72–84.

MORRISON, S. F., ERNSBERGER, P., MILNER, T. A., CALLAWAY, J., GONG, A. & REIS, D. J. (1989). A glutamate mechanism in the intermediolateral nucleus mediates excitatory responses to stimulation of the rostral ventrolateral medulla. *Progress in Brain Research* **81**, 159–169.

NOLAN, M. F., LOGAN, S. D. & SPANSWICK, D. (1998). Electrical synapses between rat sympathetic preganglionic neurones *in vitro. Journal of Physiology* **513.P**, 36*P.*

PICKERING, A. E., SPANSWICK, D. & LOGAN, S. D. (1991). Whole-cell recordings from sympathetic preganglionic neurons in rat spinal cord slices. *Neuroscience Letters* **130**, 237–242.

REKLING, J. C. & FELDMAN, J. L. (1997). Bidirectional electrical coupling between inspiratory motoneurons in the newborn mouse nucleus ambiguus. *Journal of Neurophysiology* **78**, 3508–3510.

SPANSWICK, D. & LOGAN, S. D. (1990). Spontaneous rhythmic activity in the intermediolateral cell nucleus of the neonatal rat thoracolumbar spinal cord *in vitro. Neuroscience* **39**, 395–403.

SPANSWICK, D., RENAUD, L. P. & LOGAN, S. D. (1998). Bilaterally evoked monosynaptic EPSPs, NMDA receptors and potentiation in rat sympathetic preganglionic neurones *in vitro. Journal of Physiology* **509**, 195–209.

SPRAY, D. C. (1996). Physiological properties of gap junction channels in the nervous system. In *Gap Junctions in the Nervous System*, ed. SPRAY, D. C. & DERMIETZEL, R., pp. 39–59. Springer-Verlag, Heidelberg.

SPRUSTON, N., JAFFE, D. B., WILLIAMS, S. H. & JOHNSTON, D. (1992). Voltage and space clamp errors associated with measurement of electrotonically remote synaptic events. *Journal of Neurophysiology* **70**, 781–802.

TRAUB, R. D. (1995). Model of synchronized population bursts in electrically coupled interneurons containing active dendritic conductances. *Journal of Computational Neuroscience* **2**, 283–289.

VIGMOND, E. J., PEREZ VALAZQUEZ, J. L., VALIANTE, T. A., BARDAKJIAN, B. L. & CARLEN, P. L. (1997). Mechanisms of electrical coupling between pyramidal cells. *Journal of Neurophysiology* **78**, 3107–3116.

WELSH, J. P. & LLINÁS, R. (1997). Some organizing principles for the control of movement based on olivocerebellar physiology. *Progress in Brain Research* **114**, 449–461.

ZAMPIGLUI, G. A., HALL, J. E. & KREMAN, M. (1985). Purified lens junctional protein forms channels in planar lipid films. *Proceedings of the National Academy of Sciences of the USA* **82**, 8468–8472.

ZHANG, Q. Z. & HATTON, G. I. (1988). Direct evidence for electrical coupling among rat supraoptic neurons. *Brain Research* **463**, 47–56.

Corresponding author

D. Spanswick: Department of Biomedical Sciences, Institute of Medical Sciences, University of Aberdeen, Foresterhill, Aberdeen AB25 2ZD, UK.

Email: d.spanswick@abdn.ac.uk